

Forced vibration analysis of damped beam structures with composite cross-section using Timoshenko beam element

S.G. Won¹, S.H. Bae¹, W.B. Jeong^{*1}, J.R. Cho^{1a} and S.R. Bae²

¹School of Mechanical Engineering, Pusan National University, Busan 609-735, Korea

²Agency for Defense Development, Jinhae 645-016, Korea

(Received March 8, 2011, Revised May 2, 2012, Accepted May 17, 2012)

Abstract. A damped Timoshenko beam element is introduced for the DOF-efficient forced vibration analysis of beam-like structures coated with viscoelastic damping layers. The rotary inertia as well as the shear deformation is considered, and the damping effect of viscoelastic layers is modeled as an imaginary loss factor in the complex shear modulus. A complex composite cross-section of structures is replaced with a homogeneous one by means of the transformed section approach in order to construct an equivalent single-layer finite element model capable of employing the standard C^0 -continuity basis functions. The numerical reliability and the DOF-efficiency are explored through the comparative numerical experiments.

Keywords: multi-layered damped beam structure; damped Timoshenko beam element; forced vibration analysis; complex shear modulus; transformed section method

1. Introduction

Viscoelastic materials are being widely used in a variety of engineering applications for dissipating the structural vibration energy in various manners and forms, such as submarine and gun tube of tracked vehicle (Kiehl and Wayne Jerzak 2001, Dylejko *et al.* 2007, Yan *et al.* 2007). Almost all elastic structures exhibit very small damping so that their structural vibrations caused by various internal or/and external sources may produce the undesired noise as well as the unexpected structural dynamic instability. One critical situation is the underwater noise by the structural vibration of submarine for which the sound maneuvering becomes one of important requirements (Gargouri *et al.* 1998). In such a situation, a useful passive technique for reducing the underwater noise is to coat the viscoelastic material layers over the surfaces of critical elastic members such as beam-, plate- and shell-like structures showing the major contribution to the underwater noise (Sainsbury and Masti 2007, Liu *et al.* 2009).

Introducing viscoelastic layers to the elastic members under forced vibration motion gives rise to

*Corresponding author, Professor, E-mail: wbyeong@pusan.ac.kr

^aVice Director of Research and Development Institute of Midas IT Co. Ltd.

high damping effect, according to the dissipation of the vibratory flexural bending energy of the elastic member via the high distortional deformation, mostly the shear deformation of the viscoelastic material (Ruzicka 1965, DiTaranto 1965), The bending vibration of a damped sandwich structure is characterized by a combination of the oscillating flexural bending of elastic members and the alternating distortional deformation of viscoelastic layers. A large amount of research efforts have been continuously and intensively progressed since the late 1950s on the theoretical and numerical studies of the sandwich structures with viscoelastic layers, and the reader may refer to Kosmatka and Liguore (1993), Baburaj and Matsuzaki (1993), Adhikari (2000) for the extensive literature survey.

Most of the theoretical studies have been motivated by the work of Ross *et al.* (1959), called the RKU (Ross-Kerwin-Ungar) theory, who laid down the basic theoretical framework for the damped sandwich structures and derived an effective, complex, flexural stiffness of the beam cross-section with the three-layer sandwich beam model with a core viscoelastic layer. Based upon the RKU theory, DiTaranto (1965), Mead and Markus (1969), Nakra (1996) derived the partial differential equations (six order for the three layered system) for analyzing the vibration damping driven by the shear deformation of the core viscoelastic layer by introducing a complex shear modulus expressed in terms of an imaginary loss factor. These equations are thought as an extension of Euler beam theory to laminated beam-like structures with viscoelastic layers, so the problem domain is reduced to the reference axis like the neutral axis of structures (Cho and Oden 1996a, b). Thereafter, the extensive research efforts have been focused to refine, by including additional damping effects by the extensional/compressive deformation and rotary inertia, and to extend the earlier works to multi-layered systems or engineering applications, by many subsequent investigators such as Miles and Reinhall (1986), Cupial and Niziol (1995), Kiehl and Jerzak (2001), Yadav (2008).

The use of 3-D full elasticity-based finite element models like the multi-layer finite element model (Zapfe and Lesieutre 1999, Chen and Chan 2000) which are incorporated with a suitable complex elastic modulus provides the realistic vibration behavior of damped sandwich structures. But, its critical demerit is the need of too many finite elements such that the total CPU time becomes highly time-consuming when either the layer number increases or the analysis problem becomes large-scale and complex. This situation becomes more crucial as the damping layer becomes thinner, because the mesh density is strongly affected by the smallest thickness dimension (Chen and Chan 2000, Xie and Steve Shepard 2009). The finite element implementation of the RKU theory can be a possible solution from the fact that the vibration damping behavior is expressed definitely by the transverse displacement of the reference axis (or surface) of structure. However, the derivation of high-order PDE and the corresponding high-order Hermitian basis functions become troublesome as the layer number increases, together with the difficulty in identifying the appropriate boundary conditions (Mead and Markus 1969). In this context, an equivalent single-layer finite element model which can be a sort of classical beam theory for laminated elastic composites is preferable.

The goal of the current study is to introduce a damped Timoshenko beam element for analyzing the multi-layered damped beam-like structures with composite cross-section with the minimum degrees of freedom. The effective material properties of damped structures coated with viscoelastic layers are derived by the transformed section method (Moy and Nikoukar 2002, Colombi and Poggi 2006), and the standard C^0 -continuity basis functions are employed. The rotary inertia as well as the shear deformation of the entire structure is taken into consideration. The damping effect of the viscoelastic material is reflected into the shear modulus in the manner of a complex modulus with

an imaginary loss factor. The numerical results verifying the DOF-efficiency as well as the numerical reliability are also presented.

2. Problem description

2.1 Multi-layered damped beam-like structures

Fig. 1(a) depicts a three-layered damped beam-like structure with an elastic core layer which is used to dissipate the vibration energy of various structural components of submarine. However, for the current study, the core layer does not need to be elastic and the layer number and the cross-section shape are arbitrary, as well the viscoelastic layers are thinner than the core elastic layer. Each material layer is assumed to be homogeneous, isotropic and linearly elastic obeying the Hooke's law and its mechanical properties are temperature and frequency independent. As well, the interfaces between layers are perfectly bonded such that slip, overlap and gap at the interfaces are not allowed, and the total composite thickness is small in comparison with the characteristic length of the entire structure.

The flexural vibration of elastic layer causes the significant shear deformation of viscoelastic layers, which takes charge of the major portion of the total vibration energy dissipation of the damped sandwich structure. Based upon this mechanical vibration feature, earlier investigators such as Ross *et al.* (1959), DiTaranto (1965) introduced a constrained-layer damping theory in which the whole damping is represented by only the shear deformation of viscoelastic layers, by ignoring other effects such as the shear deformation of elastic layers, the longitudinal strains of viscoelastic layers, and the transverse normal strains in both elastic and viscoelastic layers. Where, the shear deformation-induced damping is taken into consideration by means of the complex shear modulus $G^* = G(1 + i\eta)$ of viscoelastic layers with η being the loss factor. Using the fundamental relations of the elementary beam theories, one can derive a set of partial differential equations governing the lateral dynamic displacement $w(x;t)$ of the entire sandwich structure and the longitudinal displacement $u(x;t)$ of the reference axis. Furthermore, the relation between $u(x;t)$ and $w(x;t)$ leads to a higher order partial differential dynamic equation for $w(x;t)$. The reader may refer to Yadav (2008) for more details.

On the other hand, Fig. 1(b) shows an equivalent single-layer finite element model for the current study, which is based upon the Timoshenko beam theory (Timoshenko 1955, Bambill *et al.* 2010). Where, the reference axis and the superscript $(\cdot)^*$ indicate the neutral axis of the damped structure and the complex values respectively, and the elastic constants ρ , G^* and $(EI_y)^*$ are the equivalent

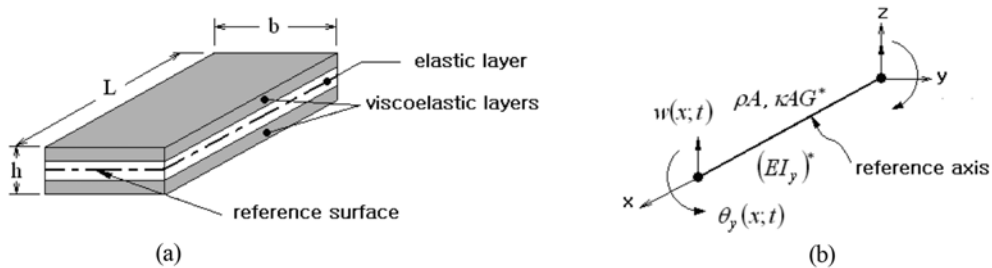


Fig. 1 (a) Three-layered damped beam structure and (b) equivalent damped Timoshenko beam model

values in the area-averaged sense (Cho and Oden 2000). Both the neutral axis and the equivalent elastic constants are determined by the transformed-section method which will be fully described in Section 3. Employing the Timoshenko beam theory implies that both the shear deformation and the rotary inertia not only of the viscoelastic layers but of the elastic layers are taken into consideration.

2.2 Forced vibration of damped Timoshenko beam

Referring to Fig. 1(b), the total strain energy U stored within a Timoshenko beam of length L due to both the bending and shear deformations is given by

$$U(t) = \frac{1}{2} \int_0^L [(EI_y)^* \theta_{y,x}^2 + \kappa AG^* (w_{,x} - \theta_y)^2] dx \quad (1)$$

where G^* and A are the equivalent complex shear modulus and the cross-section area of the beam respectively, and $(EI_y)^*$ is the equivalent complex flexural rigidity of the beam about the neutral axis. In addition, κ ($\kappa = 5/6$) is the shear correction factor, and θ_y and $(w_{,x} - \theta_y)$ are the slope of the neutral axis and the transverse shear strain respectively. Although the correction factor is in function of the cross-section shape (Cowper 1996) and the vibration mode, but it is assumed to be constant in the current study. Meanwhile, the total kinetic energy T due to both the lateral motion and rotary inertia of the beam is given by

$$T(t) = \frac{1}{2} \int_0^L [\rho I_y \dot{\theta}_y^2 + \rho A \dot{w}^2] dx \quad (2)$$

with the area-averaged mass density ρ of the beam and the area moment of inertia I_y about the neutral axis.

Letting W be the work done by the external load, for example the distributed load $q(x, t)$ applied to the beam at time t , the total potential energy $\Pi(t)$ at time t is written as $\Pi(t) = U(t) - W(t)$. Then, the Lagrangian functional L (Reddy 1992) at time t is defined by

$$L(w, \theta_y, \dot{w}, \dot{\theta}_y, q) = T(\dot{w}, \dot{\theta}_y) - \Pi(w, \theta_y, q) \quad (3)$$

And, the generalized Hamilton principle for a non-conservative viscoelastic dynamic system during a time period \tilde{t} is given by

$$\delta \int_0^{\tilde{t}} L(w, \theta_y, \dot{w}, \dot{\theta}_y, q) dt = 0 \quad (4)$$

Substituting Eqs. (1)-(3) into Eq. (4) and taking the variations with respect to w and θ_y lead to the following partial differential equations governing the forced vibration of the damped Timoshenko beam

$$\rho A \frac{\partial^2 w}{\partial t^2} - \frac{\partial}{\partial x} [\kappa AG^* (\frac{\partial w}{\partial x} - \theta_y)] = q(x; t) \text{ in } [0, L] \times (0, \tilde{t}] \quad (5)$$

$$\rho I_y \frac{\partial^2 \theta_y}{\partial t^2} - \kappa AG^* (\frac{\partial w}{\partial x} - \theta_y) - \frac{\partial}{\partial x} [(EI_y)^* \frac{\partial \theta_y}{\partial x}] = 0 \text{ in } [0, L] \times (0, \tilde{t}] \quad (6)$$

with two sets of the boundary conditions (Fung 1965).

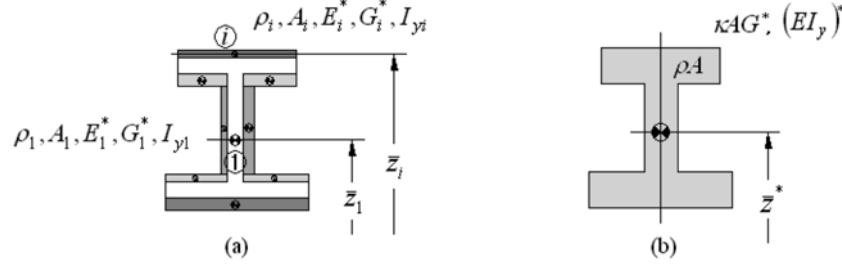


Fig. 2 (a) I-shape composite cross-section and (b) transformed homogeneous cross-section

3. Finite element approximation by utilizing the transformed section method

Fig. 2(a) depicts an I-shape composite cross-section composed of N damped and undamped elastic members with the elastic properties $\rho_i, A_i, E_i^*, G_i^*$ and I_{yi} . Note that $E_i^* = E_i$ and $G_i^* = G_i$ for the undamped members. Its transformed cross-section with the homogeneous elastic material constants is represented in Fig. 2(b), where \bar{z}^* indicates the complex neutral axis of the cross-section.

The equivalent elastic constants (ρA) , $(\kappa A G^*)$, (ρI_y^*) and $(EI_y)^*$ of the transformed section which are included in Eqs. (5) and (6) are calculated in the area-averaged sense (Cho and Oden 2000)

$$\int_A (\cdot) dA = \sum_{i=1}^N \int_{A_i} (\cdot)_{A_i} dA \quad \text{or} \quad (\cdot) = \frac{1}{|A|} \sum_{i=1}^N \int_{A_i} (\cdot)_{A_i} dA \quad (7)$$

For example, the complex flexural rigidity $(EI_y)^*$ of the transformed cross-section A is expressed as an algebraic sum of those of each layer such that

$$(EI_y)^* = E_1^*(I_y^*)_{A_1} + \dots + E_N^*(I_y^*)_{A_N} = E_1^*(I_{y1} + d_1^{*2} A_1) + \dots + E_N^*(I_{yN} + d_N^{*2} A_N) \quad (8)$$

where $d_i^* = \bar{z}_i - \bar{z}^*$ and $(I_{yi}^*)_{A_i}$ are the complex moments of inertia of each layer. The neutral axis \bar{z}^* of the transformed cross-section A is calculated from the axial force equilibrium (Fung 1965)

$$\int_{A_1} \sigma_x^* dA + \dots + \int_{A_N} \sigma_x^* dA = 0 \quad (9)$$

Substituting $(\sigma_x^*)_{A_i} = E_i^*(\varepsilon_x^*)_{A_i} = k E_i^* \zeta^*$ (k -the curvature of the neutral axis) into Eq. (9), together with $\zeta^* = z - \bar{z}^*$ and $n_i^* = E_i^*/E_1^*$, provides us

$$\bar{z}^* = \frac{\sum_{i=1}^N n_i^* \bar{z}_i A_i}{\sum_{i=1}^N n_i^* A_i} \quad (10)$$

where \bar{z}_i is the neutral axis of the i -th layer in the damped beam structure.

In order for the finite element approximation, we divide the reference axis into a finite number of elements and introduce iso-parametric C^0 basis functions $\phi_i(x)$ to two state variables

$$w^h(x, t) = \sum \phi_i(x) \bar{w}_i(t) = \Phi(x) \cdot \bar{\mathbf{w}}(t) \quad (11)$$

$$\theta_y^h(x, t) = \sum \phi_i(x) \bar{\theta}_{yi}(t) = \Phi(x) \cdot \bar{\theta}_y(t) \quad (12)$$

Substituting Eqs. (11) and (12) into the variational forms of Eqs. (5) and (6) results in a complex linear equation system given by

$$\begin{bmatrix} \mathbf{M}_{ww} & 0 \\ 0 & \mathbf{M}_{\theta\theta}^* \end{bmatrix} \begin{Bmatrix} \ddot{\bar{\mathbf{w}}}(t) \\ \ddot{\bar{\theta}}_y(t) \end{Bmatrix} + \begin{bmatrix} \mathbf{K}_{ww}^* & \mathbf{K}_{w\theta}^* \\ \mathbf{K}_{\theta w}^* & \mathbf{K}_{\theta\theta}^* \end{bmatrix} \begin{Bmatrix} \bar{\mathbf{w}}(t) \\ \bar{\theta}_y(t) \end{Bmatrix} = \begin{Bmatrix} \mathbf{f}_w \\ \mathbf{0} \end{Bmatrix} \quad (13)$$

with matrices defined by

$$\mathbf{M}_{ww} = \int_0^L (\rho A \Phi^T \Phi) dx \quad (14)$$

$$\mathbf{M}_{\theta\theta}^* = \int_0^L (\rho I_y^* \Phi^T \Phi) dx \quad (15)$$

$$\mathbf{K}_{ww}^* = \int_0^L [\kappa A G^* (\nabla \Phi)^T (\nabla \Phi)] dx \quad (16)$$

$$\mathbf{K}_{w\theta}^* = \int_0^L [-\kappa A G^* (\nabla \Phi)^T \Phi] dx \quad (17)$$

$$\mathbf{K}_{\theta\theta}^* = \int_0^L [\kappa A G^* \Phi^T \Phi + (EI_y)^* (\nabla \Phi)^T (\nabla \Phi)] dx \quad (18)$$

$$\mathbf{f}_w = \int_0^L \Phi^T q dx \quad (19)$$

Denoting $\{\bar{\mathbf{w}}(t), \bar{\theta}_y(t)\}^T$ be $\bar{\mathbf{u}}(t)$, the above equation system (13) can be rewritten in a concise form given by

$$[\mathbf{M}^*] \ddot{\bar{\mathbf{u}}}(t) + [\mathbf{K}^*] \bar{\mathbf{u}}(t) = \{\mathbf{F}\} \quad (20)$$

For a simple sinusoidal external force $q(x, t) = \bar{q}(x) e^{i\tilde{\omega}t}$, the corresponding load vector $\{\mathbf{F}\} = \{\bar{\mathbf{F}}\} e^{i\tilde{\omega}t}$ and the dynamic response $\bar{\mathbf{u}}(t) = \bar{\mathbf{U}} e^{i\tilde{\omega}t}$ transforms Eq. (20) into a complex linear equation system expressed in terms of the external excitation frequency

$$\{[\mathbf{K}^*] - \tilde{\omega}^2 [\mathbf{M}^*]\} \bar{\mathbf{U}} = \{\bar{\mathbf{F}}\} \quad (21)$$

Then, the frequency response $\bar{\mathbf{U}}$ to a given excitation frequency $\tilde{\omega}$ can be obtained using the inverse matrix $[\mathbf{H}^{-1}]$ as

$$\bar{\mathbf{U}} = [\mathbf{H}^{-1}(\tilde{\omega})] \{\bar{\mathbf{F}}\}, \quad [\mathbf{H}^{-1}(\tilde{\omega})] = [\mathbf{K}^*] - \tilde{\omega}^2 [\mathbf{M}^*] \quad (22)$$

4. Numerical experiments

A test FEM program was coded in Fortran according to the finite element formulation described in Section 3, for which a direct solver of complex matrices was employed to solve the frequency response. Three numerical examples are considered to illustrate the validity and the DOF-efficiency of the proposed element; a three-layered damped cantilever beam of rectangular section and two beam-like damped slender structures with three-layered *I*-shape cross-section. The detailed

Table 1 Material properties taken for the numerical experiments

Parameters	Steel	Rubber
Density ρ (N/m ³)	7,850	2,000
Young's modulus E (N/m ²)	2.1×10^{11}	1.0×10^9
Shear modulus G (N/m ²)	8.08×10^{10}	3.36×10^8
Poisson's ratio ν	0.3	0.49
Loss factor η	0	0.49

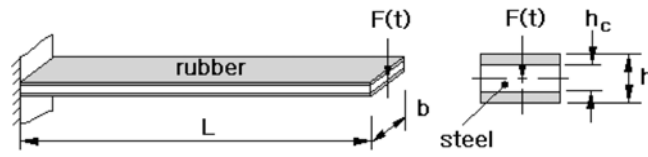


Fig. 3 A three-layered composite cantilever beam composed of steel and rubber (unit: mm)

geometries and dimensions will be given later, and steel is taken for a core layer while rubber for two outer layers. Material properties of two base materials and the major parameters are recorded in Table 1, where the loss factor η is taken variable for the parametric investigation. The shear correction factor κ is set by $5/6$ for steel and 0 for rubber. For the comparison purpose, the problems are also solved by using 2-node Euler beam elements and 8-node Nastran solid (cubic) elements.

The geometry and dimensions of the first example is shown in Fig. 3, where b , h and h_c are set by 24, 24 and 6 mm respectively while the beam length L is taken variable. A unit impulse is applied at the center of the beam cross-section at the right end and the dynamic response is measured at the same point where unit impulse is applied. The neutral axis is uniformly discretized for both the Euler and Timoshenko beam models, while the 3-D beam model is discretized with 4-node cubic Nastran solid elements such that the cross-section is divided into 8×8 ($2 + 4 + 2$ in the thickness direction) and the division number in the axial direction is the same as the Euler and Timoshenko models. With this model, the convergence with the respect to the total number of elements and the variation to the beam slenderness of the frequency response are examined.

The frequency responses of the damped cantilever beam for four different mesh densities are comparatively represented in Fig. 4, for which the beam length L is set by 70 mm. Note that the element number means the division number along the neutral axis. The relative beam thickness is taken large such that the difference among three models is clearly observed. One can clearly observe that the difference in the frequency responses of three models becomes larger as the frequency goes higher, but the frequencies and receptances of each model show the clear convergence with respect to the element number. It can be clearly found from Table 2 where the frequencies and the receptances of three lowest peaks are recorded. The frequencies of Timoshenko and 3-D solid models are lower-bounded, showing the typical convergence characteristic of the standard displacement-based formulation (Szabo and Babuska 1991). But, the first and second frequencies of Euler model are upper-bounded. One can observe that the Timoshenko model provides the frequencies closer to those of the 3-D solid model. Meanwhile, three models show the remarkable difference in the receptances such that the Timoshenko model exhibits the highest

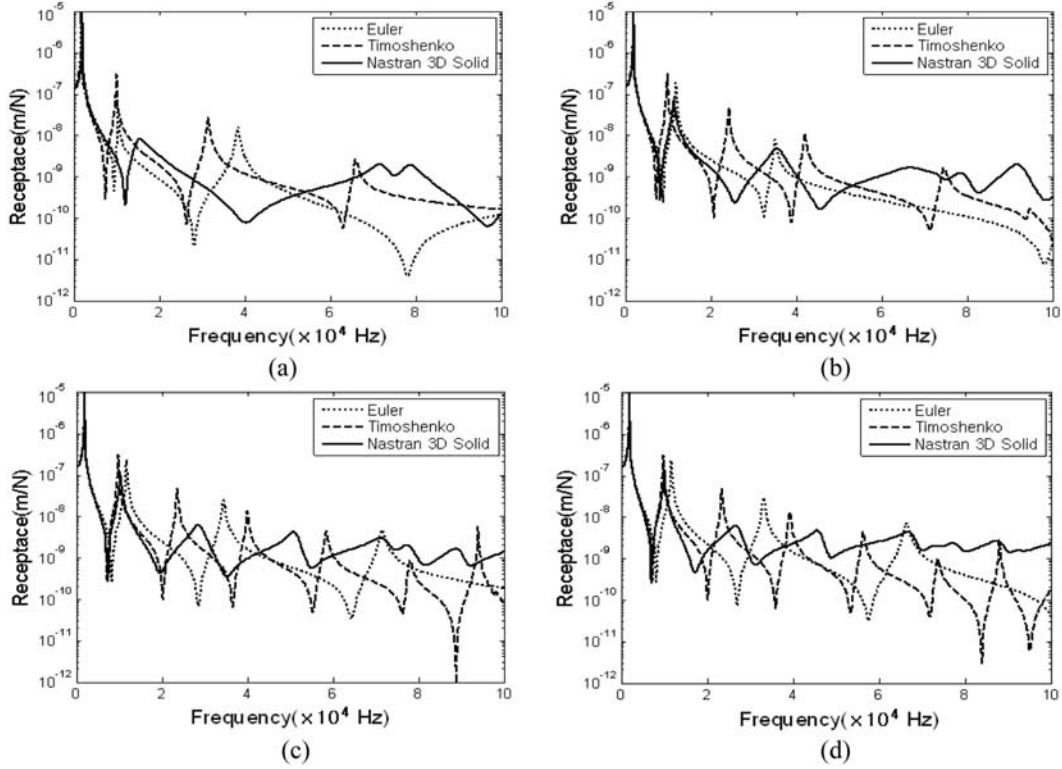


Fig. 4 Convergence of FRF to the element number: (a) two, (b) four, (c) eight and (d) sixteen

Table 2 Convergence of the frequency response to the element number

Peaks	Element number	Frequency (Hz)			Receptance (m/N)		
		Euler	Timoshenko	Solid	Euler	Timoshenko	Solid
1st	2	1,681	1,805	1,968	9.575E-6	9.859E-6	5.292E-6
	4	1,815	1,803	1,891	9.447E-6	9.849E-6	7.025E-6
	8	1,847	1,803	1,854	9.387E-6	9.847E-6	8.071E-6
	16	1,854	1,803	1,839	9.336E-6	9.845E-6	8.503E-6
	32	1,856	1,803	1,834	9.363E-6	9.844E-6	8.635E-6
2nd	2	10,390	9,967	15,430	4.742E-8	3.020E-6	8.092E-9
	4	11,840	9,822	11,380	1.835E-7	3.067E-7	7.421E-8
	8	11,760	9,772	10,300	2.269E-7	3.060E-7	1.184E-7
	16	11,670	9,758	10,020	2.358E-7	3.059E-7	1.320E-7
	32	11,650	9,755	9,939	2.378E-7	3.058E-7	1.355E-7
3rd	2	38,350	31,380	71,760	1.567E-8	2.699E-8	1.990E-9
	4	35,060	24,180	35,500	7.773E-8	4.634E-8	4.794E-9
	8	34,370	23,560	28,430	2.481E-8	4.649E-8	6.244E-9
	16	33,120	23,400	26,560	2.921E-8	4.638E-8	6.222E-9
	32	32,730	23,350	26,020	3.014E-8	4.634E-8	6.449E-9

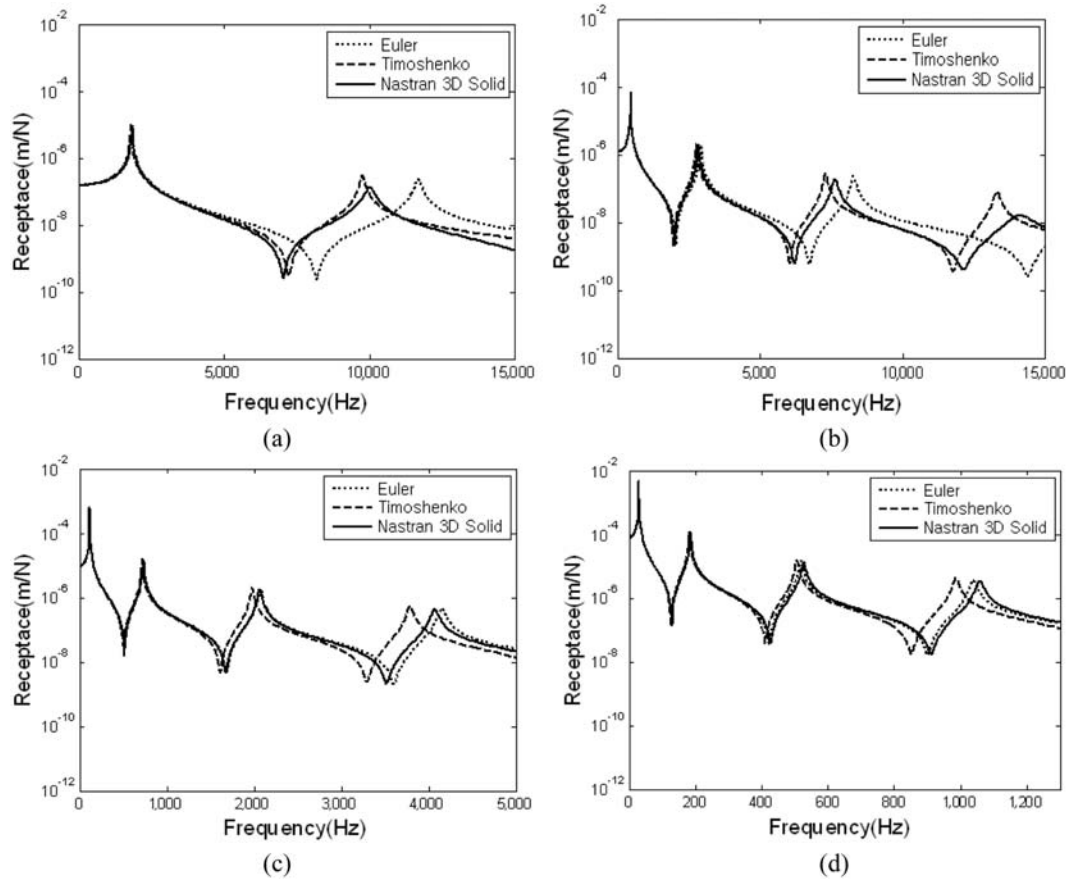


Fig. 5 Variation to the relative thickness ratio: (a) $L/h = 70/24$, (b) $L/h = 140/24$, (c) $L/h = 280/24$ and (d) $L/h = 560/24$

dynamic flexibility and vice versa for the 3-D solid model. It is observed that the receptances of 3-D solid model are sensitive to the total number of elements such that finer mesh is required to obtain more converged receptances. But, the element partition number along the beam axis is kept the same as Euler and Timoshenko beam models for the consistent comparative investigation of convergence characteristics.

Fig. 5 represents the frequency responses of three models for four different thickness ratios of the beam, for which the beam length L is taken variable while the beam thickness $h = 24$ mm is kept unchanged. Regardless of the beam length, the mesh density is kept constant such that the division density in the axial direction is 16 elements per 70 mm for all the three models and the cross-section of solid model is uniformly discretized by 8×8 . It is clearly observed that the Timoshenko model shows the frequency response closer to one by the 3-D solid model, when compared with the Euler model. However, the difference in the frequency responses of three models becomes smaller in proportion to the beam slenderness such that the Timoshenko and 3-D solid models approach the Euler model which serves as a limit theory of 3-D linear elastic beam problems (Cho and Oden 1996, Szabo and Babuska 1991).

The detailed frequencies and receptances of four lowest peaks of three models are compared in

Table 3 Variation of the frequency response to the beam slenderness

L/h	Peaks	Frequency (Hz)			Receptance (m/N)		
		Solid	Euler	Timoshenko	Solid	Euler	Timoshenko
70/24	1st	1,839	1,854	1,803	8.494E-6	9.336E-6	9.845E-6
	2nd	10,010	11,670	9,758	1.281E-7	2.358E-7	3.059E-7
	3rd	26,900	33,120	23,400	4.227E-9	2.921E-8	4.638E-8
	4th	85,580	66,300	39,160	1.296E-7	7.218E-9	1.325E-8
140/24	1st	467	464	461	6.710E-5	7.448E-5	7.558E-5
	2nd	2,838	2,919	2,766	1.823E-6	1.886E-6	2.053E-6
	3rd	7,628	8,279	7,297	1.919E-7	2.337E-7	2.830E-7
	4th	14,110	16,580	13,310	1.642E-8	5.773E-8	8.047E-8
280/24	1st	117	116	116	5.219E-4	5.959E-4	5.910E-4
	2nd	734	730	718	1.388E-5	1.506E-5	1.555E-5
	3rd	2,060	2,070	1,976	1.774E-6	1.869E-6	2.031E-6
	4th	4,063	4,144	3,782	4.459E-7	4.619E-7	5.465E-7
	5th	6,777	7,048	6,082	1.554E-7	1.4808E-7	2.077E-7
560/24	1st	29	29	29	2.613E-3	4.767E-3	4.797E-3
	2nd	185	182	181	1.210E-4	1.162E-4	1.079E-4
	3rd	526	517	505	1.353E-5	1.487E-5	1.573E-5
	4th	1,056	1,036	984	3.408E-6	3.696E-6	4.143E-6
	5th	1,805	1,762	1,614	1.184E-6	1.243E-6	1.535E-6
1,120/24	1st	7	7	7	6.558E-3	8.939E-3	8.653E-3
	2nd	46	46	45	6.182E-4	6.504E-4	6.286E-4
	3rd	132	129	127	1.026E-4	1.127E-4	1.248E-4
	4th	267	259	249	2.627E-5	2.956E-5	3.208E-5
	5th	459	441	410	8.990E-6	9.898E-6	1.196E-5

Table 3 for five different thickness ratios. The 3-D solid and Timoshenko models provide the frequencies remarkably different from those of the Euler model at $L/h = 70/24$, and the difference becomes larger as the peak frequency becomes higher. But, it is clearly shown that this difference becomes smaller in proportion to the beam slenderness, and this trend becomes apparent for the peaks with lower frequencies. Meanwhile, three models show the remarkable difference in the receptances regardless of the beam slenderness such that the Timoshenko model exhibits the highest dynamic flexibility and vice versa for the 3-D solid model. Furthermore it is observed that the difference does not become smaller in proportion to the beam slenderness.

Next, we apply the damped Timoshenko beam element to the beam-like slender structures of I -shape cross-section coated with viscoelastic layers shown in Fig. 6. While the previous experiments were aimed at examining the reliability of the damped beam element by comparing the Euler beam element with 3-D Nastran solid element, next two experiments are performed in order to examine the DOE-efficiency as well as the numerical accuracy of the damped beam element. As in the previous experiments, the material properties given in Table 1 except for the loss factor are kept

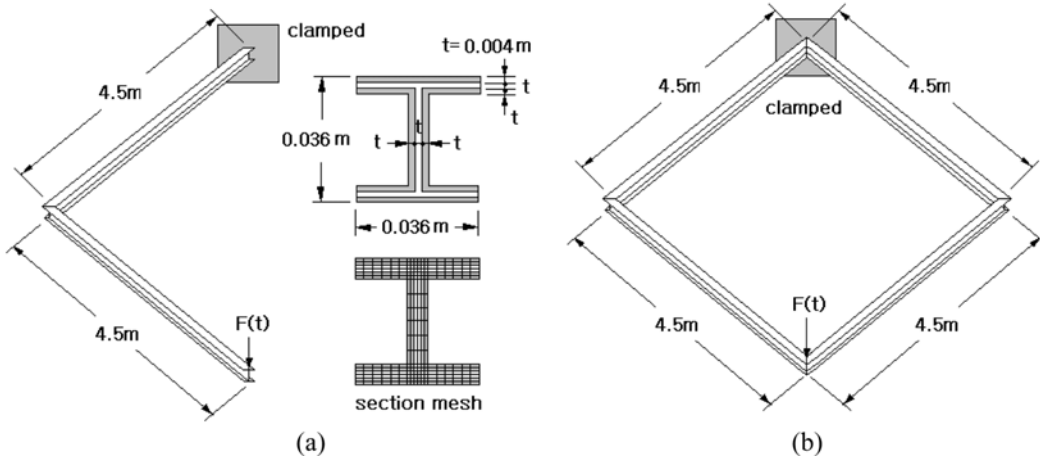


Fig. 6 Damped beam-like slender structures with *I*-shape cross-section: (a) *L*-shape and (b) closed-rectangle

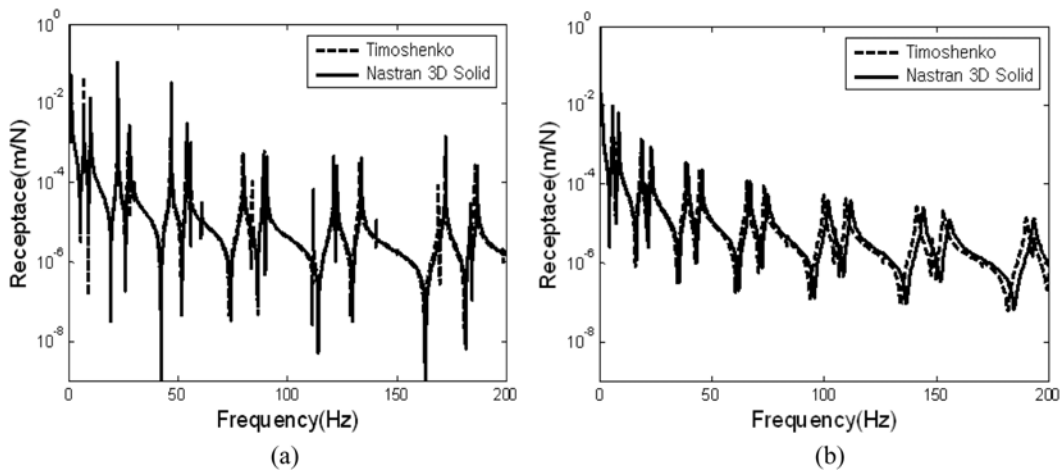


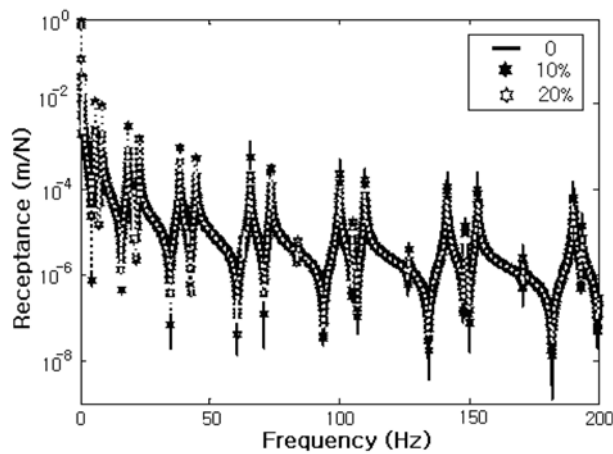
Fig. 7 Frequency responses of the *L*-shape structure: (a) undamped and (b) damped

unchanged. Two beam structures are uniformly divided with the mesh density of 2 elements/10 mm along the neutral axis. Meanwhile the cross-section of the 3-D solid model is discretized by $18 \times 18 - 2 \times (6 \times 6)$ such that each layer is uniformly divided by two in the thickness direction. Note that $2 \times (6 \times 6)$ indicates the element numbers for the left and right void regions in the convex hull of the *I*-shape cross-section.

Fig. 7 compares the frequency responses of the *L*-shape structure between the Timoshenko beam element and 3-D Nastran solid element, where the damped responses are obtained with the loss factor η of 0.49. For both models, a unit impulse is applied at the center of the beam cross-section at the right end, where the frequency responses are also measured. The undamped frequency response obtained by the damped Timoshenko beam elements shows a good agreement with one obtained by 3-D Nastran solid elements, except for the small discrepancy at higher frequencies. Meanwhile, the damped frequency response by the damped Timoshenko beam elements follows well the damped frequency response by 3-D Nastran solid elements such that the difference between

Table 4 Variation of the frequency response of the *L*-shape structure to the loss factor

Loss factor (%)	Receptance (m/N)		
	1st peak ($\times 10^{-2}$)	2nd peak ($\times 10^{-2}$)	3rd peak ($\times 10^{-3}$)
0	4.160	1.179	9.498
5	4.160	1.175 (-0.339%)	9.434 (-0.674%)
10	4.160	1.167 (-1.018%)	9.247 (-2.643%)
15	4.160	1.148 (-2.629%)	8.959 (-5.675%)
20	4.160	1.125 (-4.580%)	8.598 (-9.476%)

Fig. 8 Variation of the frequency response to the loss factor (*L*-shape structure)

two responses are not distinguished up to the eighth peak.

The receptances of three lowest peaks to the loss factor which are obtained using the damped Timoshenko beam elements are recorded in Table 4, where the values in parenthesis indicate the relative changes with respect to the receptances of the peaks at $\eta = 0$. For reference, frequencies of three lowest peaks are 0.938, 5.820 and 8.380 Hz respectively. The receptance variation of the first peak is too small to distinguish within three decimal places, but the effect of the loss factor on the receptance increases as the resonance frequency becomes higher. The decrease of the receptance in proportion to the loss factor is clearly shown in Fig. 8 such that the *L*-shape damped beam structure exhibits more sensitive frequency response to the loss factor at higher peaks.

Fig. 9 represents the undamped and damped frequency responses of the closed-rectangle structure which are obtained using the damped Timoshenko beam and 3-D Nastran solid elements respectively. As in the previous *L*-shape beam structure, a unit impulse is applied at the center of the beam cross-section as shown in Fig. 6(b). The frequency responses are taken at the same point where the unit impulse is applied, and the damped responses are obtained with the loss factor equal to 0.49. One can observe that the difference in the undamped frequency responses between two elements is small and the damped frequency response obtained by the damped Timoshenko beam element follows well one obtained by 3-D Nastran solid element up to seventh peak. When compared with the *L*-shape beam structure, the difference in the undamped and damped frequency responses between two different finite elements is more noticeable. It implies that the closed-

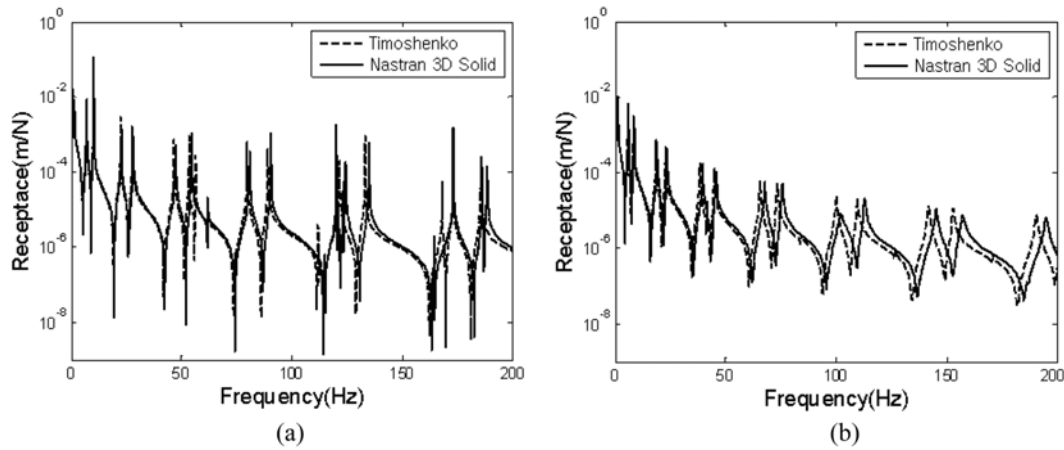


Fig. 9 Frequency responses of the closed rectangular structure: (a) undamped and (b) damped

Table 5 Variation of the frequency response of the closed-rectangle structure to the loss factor (Timoshenko)

Loss factor (%)	Receptance (m/N)		
	1st peak ($\times 10^{-2}$)	2nd peak ($\times 10^{-2}$)	3rd peak ($\times 10^{-3}$)
0	5.550	3.229	4.802
5	5.550	2.965 (-8.176%)	4.769 (-0.687%)
10	5.550	2.446 (-24.250%)	4.672 (-2.707%)
15	5.550	1.976 (-38.805%)	4.523 (-5.810%)
20	5.550	1.621 (-49.799%)	4.337 (-9.683%)

rectangle beam structure exhibits the more complex structural vibration than the *L*-shape beam structure. Through the comparison of the undamped and damped frequency responses of two beam problems between the damped Timoshenko and 3-D Nastran solid elements, it has been clearly confirmed that the proposed damped beam element accurately analyzes the frequency response of extremely long slender damped sandwich beam structures with complex cross-section.

Table 5 represents the receptances of three lowest peaks of the closed-rectangle beam structure with respect to the loss factor, where the frequencies of three lowest peaks are 0.973, 5.885 and 8.442 Hz respectively. The decrease of the receptance in proportion to the loss factor is clearly shown in Fig. 10. As in the previous *L*-shape beam structure, the dependence of the first peak receptance on the loss factor is too small to distinguish within three decimal places. However, differing from the *L*-shape beam structure, the second peak is more sensitive to the loss factor than the third peak. This difference between two beam structures can be also observed by comparing Fig. 8 with Fig. 9. It implies that the inherent dynamic characteristic of the closed-rectangle beam is different from one of the *L*-shape beam structure.

The total numbers of elements and degrees of freedom required to discretize three damped beam structures shown in Figs. 3 and 6 are compared in Table 6. It should be noted that these numbers are calculated based on the mesh density of 16 elements/70 mm in the axial direction and the previous element numbers used to discretize the rectangle and *I*-shape cross-sections of the beam. It

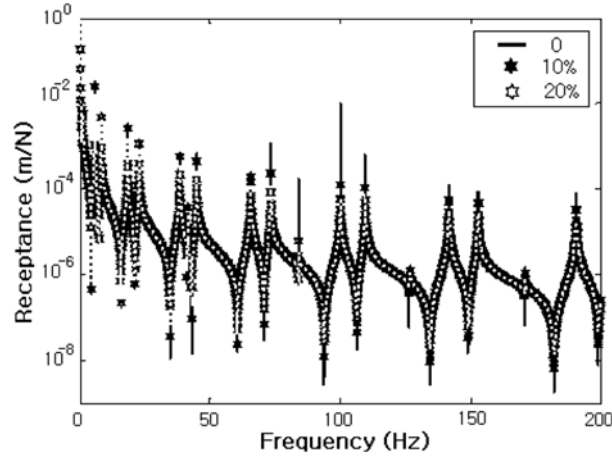


Fig. 10 Variation of the frequency response to the loss factor (closed-rectangle structure)

Table 6 Comparison of degrees of freedom

Problem type	Total number of elements			Total number of DOF's		
	Solid	Euler	Timoshenko	Solid	Euler	Timoshenko
I	1,024	16 (1.56%)	16 (1.56%)	3,888	16 (0.41%)	16 (0.41%)
II	45,360	-	180 (0.40%)	167,940	-	180 (0.11%)
III	90,720	-	360 (0.40%)	334,947	-	359 (0.11%)

is confirmed that the proposed Timoshenko beam element can successfully provide us the reliable frequency responses with the total element number extremely smaller than 3-D solid element.

5. Conclusions

A damped Timoshenko beam element has been introduced aiming at the DOF-efficient forced vibration analysis of multi-layered damped beam-like structures with composite cross-section. The damping effect of viscoelastic layers were taken into consideration by means of the complex shear modulus and the equivalent mechanical properties of the composite beam cross-section were derived by the transformed section method. Through the benchmark experiments, the proposed Timoshenko beam element shows the robust convergence to the element number and provides the more accurate frequency response than the Euler beam element. As well, it has been justified from the comparison with 3-D solid element that the proposed damped beam element accurately analyzes the frequency response of the slender damped sandwich beam structures of complex cross-section with the extremely small number of elements.

Acknowledgements

This research was supported by Defense Acquisition Program Administration (DAPA) and

Agency for Defense Development (ADD) under Contract No. UD03000AD. This work was also supported by the Human Resource Development of the Korea Institute of Energy Evaluation and Planning (KETEP) Grant funded by the Korea government Ministry of Knowledge Economy (No. 20114030200070-11-1-000).

References

- Adhikari, S. (2000), *Damping Models for Structural Vibrations*, PhD Thesis, Cambridge University, Cambridge, UK.
- Baburaj, V. and Matsuzaki, Y. (1993), "A study on the material damping of thin angle-ply laminated plates", *J. Sound Vib.*, **172**(3), 415-419.
- Bambill, D.V., Felix, D.H. and Rossi, R.E. (2010), "Vibration analysis of rotating Timoshenko beams by means of the differential quadrature method", *Struct. Eng. Mech.*, **34**(2), 231-245.
- Chen, Q. and Chan, Y.W. (2000), "Integral finite element method for dynamical analysis of elastic-viscoelastic composite structures", *Comput. Struct.*, **74**, 51-64.
- Cho, J.R. and Oden, J.T. (1996), "A priori modeling error estimates of hierarchical models for elasticity problems for plate- and shell-like structures", *Math. Comput. Model.*, **23**(10), 117-133.
- Cho, J.R. and Oden, J.T. (1996), "A priori error estimates of hp-finite element approximations for hierarchical models of plate- and shell-like structures", *Comput. Meth. Appl. Mech. Eng.*, **132**, 135-177.
- Cho, J.R. and Oden, J.T. (2000), "Functionally graded material: a parametric study on thermal-stress characteristics using the Crank-Nicolson-Galerkin scheme", *Comput. Meth. Appl. Mech. Eng.*, **188**, 17-38.
- Colombi, P. and Poggi, C. (2006), "An experimental, analytical and numerical study of the static behavior of steel beams reinforced by pultruded CFRP strips", *Compos.: Part-B*, **37**, 64-73.
- Cowper, G.R. (1996), "The shear coefficient in Timoshenko's beam theory", *J. Appl. Mech.*, **33**, 335-340.
- Cupial, P. and Niziol, J. (1995), "Vibration and damping analysis of a three-layered composite plate with a viscoelastic mid-layer", *J. Sound Vib.*, **183**(1), 99-114.
- DiTaranto, R.A. (1965), "Theory of vibratory bending for elastic and viscoelastic layered finite-length beams", *J. Appl. Mech.*, **32**(Trans. ASME Series E 87), 881-886.
- Dylejko, P.G., Kessissoglou, N.J., Tso, Y. and Norwood, C.J. (2007), "Optimisation of a resonance changer to minimise the vibration transmission in marine vessels", *J. Sound Vib.*, **300**(1-2), 101-116.
- Fung, Y.C. (1965), *Foundations of Solid Mechanics*, Prentice-Hall, New Jersey.
- Gargouri, Y., Nautet, V., Wagstaff, P.R. and Giangreco, C. (1998), "A study of methods of characterizing the effects of internal noise sources on submarine flank arrays", *Appl. Acoust.*, **53**(4), 349-367.
- Kiehl, M.Z. and Wayne Jerzak, C.P.T. (2001), "Modeling of passive constrained layer damping as applied to a gun tube", *Shock Vib.*, **8**, 123-129.
- Kosmatka, J.B. and Liguore, S.L. (1993), "Review of methods for analyzing constrained-layer damped structures", *J. Aerospace Eng.*, **6**, 269-283.
- Liu, H.P., Wu, T.X. and Li, Z.G. (2009), "Theoretical modeling and effectiveness study of rail vibration absorber for noise control", *J. Sound Vib.*, **323**(3-5), 594-608.
- Mead, D.J. and Markus, S. (1969), "The forced vibration of a three-layer, damped sandwich beam with arbitrary boundary conditions", *J. Sound Vib.*, **10**(2), 163-175.
- Miles, R.N. and Reinhall, P.G. (1986), "An analytical model for the vibration of laminated beams including the effects of both shear and thickness deformation in the adhesive layer", *J. Vib. Acoust. Reliab. Des.*, **108**, 56-64.
- Moy, S.S.J. and Nikoukar, F. (2002), "Flexural behaviour of steel beams reinforced with carbon fibre reinforced polymer composite", *Proceedings of the ACIC 2002, Advanced Polymer Composites for Structural Applications in Construction*, London, 195-202.
- Nakra, B.C. (1996), "Vibration of viscoelastically damped laminated structures", PhD Thesis, University of London.
- Reddy, J.N. (1992), *Energy and Variational Methods in Applied Mechanics*, John Wileys & Sons, Singapore.
- Ross, D., Ungar, E.E. and Kerwin, E.M. (1959), "Damping of plate flexural vibrations by means of viscoelastic

- laminae”, *ASME Meeting Structural Damping*, New York, 49-88.
- Ruzicka, J.E. (1965), *Structural Damping*, ASME, New York.
- Sainsbury, M.G. and Masti, R.S. (2007), “Vibration damping of cylindrical shells using strain-energy-based distribution of an add-on viscoelastic treatment”, *Finite Elem. Anal. Des.*, **43**, 175-192.
- Szabo, B. and Babuška, I. (1991), *Finite Element Analysis*, John Wiley & Sons, New York.
- Timoshenko, S.P. (1955), *Vibration Problems in Engineering*, 3rd Edition, Van Nostrand Co., New York.
- Xie, Z. and Steve Shepard, W. (2009), “Development of a single-layer finite element and a simplified finite element modeling approach for constrained layer damped structures”, *Finite Elem. Anal. Des.*, **45**, 530-537.
- Yadav, B.P. (2008), “Vibration damping using four-layer sandwich”, *J. Sound Vib.*, **317**, 576-590.
- Yan, J., Li, F.Ch. and Li, T.Y. (2007), “Vibrational power flow analysis of a submerged viscoelastic cylindrical shell with wave propagation approach”, *J. Sound Vib.*, **303**(1-2), 264-276.
- Zapfe, J.A. and Lesieutre, G.A. (1999), “A discrete layer beam finite element for the dynamic analysis of composite sandwich beams with integral damping layers”, *Comput. Struct.*, **70**, 647-666.